Tribology of Graphite and Concrete, Studied by Contact Electrical Resistance Measurement During Cyclic Compression

Xiangcheng Luo
Ph.D. Graduate Student

D. D. L. Chung
Niagara Mohawk Endowed Chair Professor

Composite Materials Research Laboratory,
State University of New York at Buffalo,
Buffalo, NY 14260-4400

The tribology of graphite and cement mortar was studied by contact electrical resistance measurement during cyclic compression. Elastic deformation and plastic deformation at asperities were distinctly observed through the reversible and irreversible decreases, respectively, of the contact resistance upon loading. Elastic deformation was dominant at the maximum stress. Plastic deformation progressed and then saturated upon stress cycling. [DOI: 10.1115/1.1353588]

Introduction

Tribology is related to the mechanical interaction of materials in contact. The consequence of the interaction can be mechanical deformation, the loss of material, the damage of material and the change of the interfacial microstructure and composition, as conventionally observed by weight loss measurement, microscopy and mechanical testing. These methods typically involve observation after rather than during the mechanical interaction, due to the experimental difficulty of observation during the interaction. Observation during the interaction is valuable for detecting the reversible and irreversible effects, whereas observation after the interaction allows detection of irreversible effects only. A nondestructive monitoring technique that provides information in real time during dynamic loading is desirable. Microscopic examination of the interface viewed at the edge cannot effectively provide interfacial information, though it can be nondestructive and be in real time. Microscopic examination of the interface surfaces after separation of the contacting elements can provide microstructural information, but it cannot be performed in real time. A nondestructive method which is amenable to observation during the mechanical interaction is electrical measurement [1–8], in this case the measurement of the contact electrical resistance of the interface.

Wear or abrasion involves subjecting each point of a surface to dynamic shear. Studies of wear or abrasion are commonly conducted by monitoring the effect over an area rather than that at a fixed point. For example, in wear testing using the pin-on-disk configuration, the tip of the pin is continuously moved against the surface of the disk, so that different points on the disk are subjected to stress at different times and the effect of dynamic shear and the stress variation within a cycle of dynamic shear at a particular point of the surface are not monitored. Even if the effect of wear or abrasion is monitored in real time, say by measuring the contact electrical resistance at the sliding contact between the pin and the disk, the monitoring does not allow correlation of the effect (say the electrical resistance) at a point with the dynamic stress at the point within a stress cycle (the dynamic stress is to be distinguished from the stress amplitude). This difficulty with wear or abrasion studies stems from the fact that wear or abrasion involves one element sliding against another, so that different points in a contact are not subjected to dynamic stress in an in-phase manner. In contrast, dynamic compression does not involve sliding, so that each point in a contact is subjected to dynamic compression in an in-phase manner, i.e., all points experience the maximum compressive stress in a cycle simultaneously and all points experience the minimum stress in a cycle simultaneously. As a result, correlation is possible between the effect (say the contact electrical resistance at the contact) and the dynamic stress during dynamic loading. This correlation allows identification of the point in a stress cycle at which certain effect occurs, and moreover allows distinction between reversible effects (effects, such as elastic deformation, which vanish upon unloading) and irreversible effects (effects, such as plastic deformation, which remain upon unloading). Therefore, by studying the effect of dynamic compression rather than dynamic shear, this paper provides new information on the tribology of engineering materials, specifically graphite and concrete. Previous tribological work involving electrical resistance measurement mainly pertained to dynamic shear, i.e., wear and friction [1–6], although static compression was also addressed [7,8].

The technique used in this work is contact electrical resistance measurement during dynamic compression below the yield stress. In involves simultaneous electrical and mechanical measurements. The technique requires that the elements in contact are electrically conducting. The contact resistance of the interface between contacting elements can be conveniently measured by using the elements as electrical leads—two for passing current and two for voltage measurement (i.e., the four-probe method), as provided by two elements (beams) that overlap at 90 deg (Fig. 1). The volume resistance of each lead was negligible compared to the contact resistance of the junction, so the measured resistance (i.e., voltage divided by current) was the contact resistance. The contact resistance multiplied by the junction area gives the contact resistivity, which is independent of the junction area and describes the structure of the interface.

Due to its electrical conductivity, thermal conductivity, oxidation resistance and wear resistance, graphite is used as an electrical contact material, particularly in sliding conditions, as encountered by brushes for electric motors and other devices and by sliding electrical contacts for trams and other electric vehicles [9–16]. To further improve the conductivity, copper impregnated graphite may be used [17,18]. Because of this application, the quality of graphite-graphite electrical contacts over time under dynamic mechanical loading is of interest. Relevant questions concern how elastic and plastic deformations at the contact interface (particularly at the asperities) affect the quality of the elec-

Contributed by the Tribology Division for publication in the ASME JOURNAL OF TRIBOLOGY. Manuscript received by the Tribology Division July 27, 2000; revised manuscript received December 6, 2000. Associate Editor: M. D. Bryant.

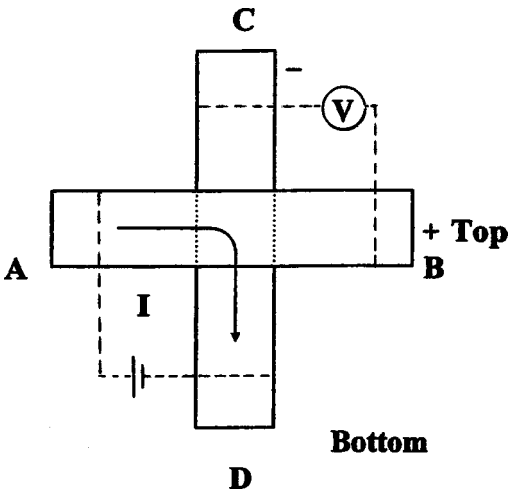

Fig. 1 Sample configuration for contact electrical resistance measurement

trical contact under mechanically loaded and unloaded conditions, and how these effects depend on the stress amplitude and the number of loading cycles.

Many concrete structures involve the direct contact of one cured concrete element with another, such that one element exerts static pressure on the other due to gravity. In addition, dynamic pressure may be exerted by live loads on the structure. An example of such a structure is a bridge involving slabs supported by columns, with dynamic live loads exerted by vehicles traveling on the bridge. Another example is a concrete floor in the form of slabs supported by columns, with live loads exerted by people walking on the floor. The interface between concrete elements that are in pressure contact is of interest, as it affects the integrity and reliability of the assembly. For example, deformation at the interface affect the interfacial structure, which can affect the effectiveness of load transfer between the contacting elements and can affect the durability of the interface to the environment. Moreover, deformation at the interface can affect the dimensional stability of the assembly. Of particular concern is how the interface is affected by dynamic loads.

In this paper, we have used contact electrical resistance measurement to monitor pressure contacts in real time during dynamic pressure application. As the surface of a material is never perfectly smooth, asperities occur on the surface, thus causing the true contact are at the interface to be much smaller than the geometric junction area. As a consequence, the local stress at the asperities is much higher than the overall stress applied to the junction. The greater the true contact area, the lower is the contact resistance. Deformation (flattening) of the asperities, as caused by the high local stress at the asperities, increases the true contact area. Increase in the number of asperities that contribute to making contact also increases the true contact area. Therefore, the interfacial structure is changed. The contact resistance provides information on the interfacial structure, particularly in relation to the deformation at the interface. By monitoring the contact resistance in real time during loading and unloading, the extent, reversibility and loading history dependence of the deformation at various points of loading and unloading can be investigated, thus providing new information on the structure and dynamic behavior of the interface.

Experimental Methods

Graphite. The graphite used in this work is electrographitic carbon of Grade EG389P (from Carbone of America Corp., Boonton, NJ). The flexural strength is 16.5 MPa, according to the manufacturer. The compressive strength is 32.6 MPa and the 0.2 percent-offset yield strength is 25.8 MPa, as measured in this work by compression testing using a rectangular sample of size 11.8×11.1 mm perpendicular to the stress direction and 12.9 mm in the stress direction and using an attached strain gage for measuring the strain in the stress direction. The electrical resistivity is $2\times10^{-3}\,\Omega.\mathrm{cm}$, the density is 1.46 g/cm^3, and the shore hardness is 30, according to the manufacturer.

The graphite was cut into rectangular strips of length 7.9–8.2 mm, width 7.0–7.8 mm and thickness 4.2 mm by using a diamond saw. The surfaces of the strips were mechanically polished by using 600-grit sandpaper, followed by washing with flowing water for the purpose of cleaning. Two strips were allowed to overlap at 90 deg to form a nearly square junction of size 7.9–8.2 mm by 7.0–7.8 mm, as illustrated in Fig. 1. The junction was the joint under study. After mechanical testing at each compressive stress amplitude (as described below), the sample surfaces were polished and cleaned again, so that testing at each stress amplitude was conducted on freshly prepared surfaces.

Concrete. This study used cement mortar (with fine aggregate but no coarse aggregate) instead of concrete (with both fine and coarse aggregates). However, the interfacial effects should be quite similar for mortar and concrete.

The cement used was Portland cement (Type I) from Lafarge Corp. (Southfield, MI). The fine aggregate used was natural sand (as passing #4 U.S. sieve, 99.9 percent SiO_2); the particle size analysis of the sand is shown in Fig. 1 of Ref. [19]; no coarse aggregate was used, and the sand/cement ratio was 1.0. The water/cement ratio was 0.35. A water-reducing agent (TAMOL SN, Rohm and Haas Co., Philadelphia, PA; sodium salt of a condensed naphthalenesulphonic acid) was used in the amount 1 percent of the cement weight.

All ingredients were mixed in a Hobart mixer with a flat beater. After pouring into molds, an external vibrator was used to facilitate compaction and decrease the amount of air bubbles. The samples were demolded after 24 h and then cured in a moist room (relative humidity=100 percent) for 28 days.

The surfaces of mortar strips had been mechanically polished by 600-grit sandpaper, in which the average abrasive SiC particle size was 25 μm. Two recangular strips of mortar of similar size and shape (90.0×14.0×13.3 mm and 95.0×14.2×13.9 mm) were allowed to overlap at 90° to form a nearly square junction (13.9×13.3 mm) as illustrated in Fig. 1. The junction was the joint under study.

Testing. Uniaxial dynamic compression was applied at the junction in the direction perpendicular to the junction, using a screw-action mechanical testing system (Sintech 2/D, Sintech, Research Triangle Park, NC), while the contact electrical resistance of the junction was measured by using a Keithley 2002 multimeter. Copper wires were applied around the strips together with silver paint to serve as electrical contacts. A DC current was applied from A to D (Fig. 1), so that the current traveled down the junction from the top strip to the bottom strip. The voltage (between B and C, Fig. 1) divided by the current yielded the contact resistance of the junction. The crosshead displacement during load cycling was typically up to 6 μm.

Results and Discussion

Graphite. Figure 2 shows the variation of the contact resistance with stress during cyclic compressive loading at a stress amplitude of 0.35 MPa. In every cycle, the resistance decreased as the compressive stress increased, such that the maximum stress corresponded to the minimum resistance and the minimum stress corresponded to the maximum resistance. During cycling, the minimum resistance (at the maximum stress) remained at the same level and the maximum resistance (at the minimum stress) did not show any systematic change. Since graphite essentially does not undergo oxidation at room temperature, the contact resistance variation is attributed to the change in contact area. Upon

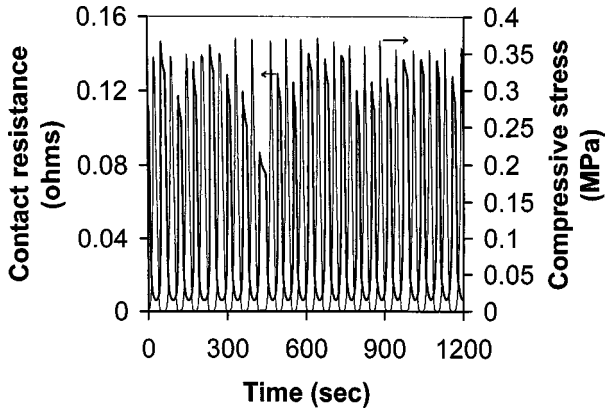

Fig. 2 Variation of contact resistance with time and of compressive stress with time during cycling compression of a graphite-graphite contact at a stress amplitude of 0.35 MPa

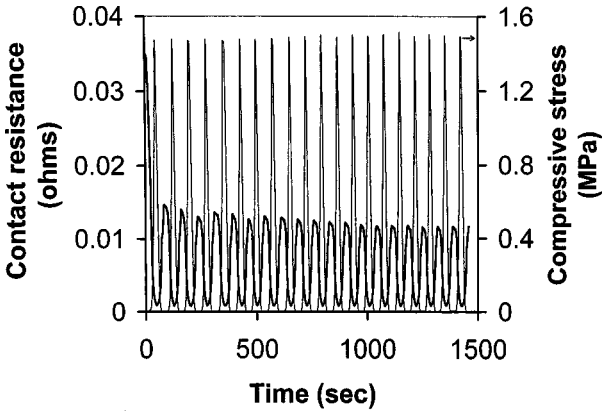

Fig. 4 Variation of contact resistance with time and of compressive stress with time during cycling compression of a graphite-graphite contact at a stress amplitude of 1.4 MPa

compressive loading, more contact area was created, thus the contact resistance decreased; upon unloading, the reverse occurred. This means that, at this stress amplitude, elastic deformation dominated the overall deformation. Although the stress at the surface asperities could be higher than the yield stress of graphite, no significant plastic deformation on the surface occurred. The contact resistance ranged from 0.007 to 0.12 Ω.

The stress amplitude in Fig. 3 is 0.7 MPa, which is higher than in that in Fig. 2. The resistance changed similarly at the two stress amplitudes, except that, in Fig. 3, the contact resistance at zero stress decreased gradually upon cycling for about eleven cycles before leveling off. The leveled-off resistance ranged from 0.002 to 0.030 Ω.

Figure 4 shows the contact resistance change at the stress amplitude of 1.4 MPa. The resistance at zero stress essentially took only the first cycle to level off. The leveled-off contact resistance ranged from 0.001 to 0.013 Ω.

The highest stress amplitude of 1.4 MPa (much lower than the yield strength 25.8 MPa) corresponded to a strain of 0.14 percent, according to the compressive stress-strain curve. For the sample thickness (4.2 mm) used for measuring the contact electrical resistance, this strain corresponded to a dimensional change (shrinkage) of 6 μm. Thus, the displacement associated with Figs. 2–4 is negligible.

Although the stress amplitudes used were all much below the yield strength, the local stress at asperities could be high enough to cause plastic deformation. The decrease of the contact resistance at zero stress in Figs. 3 and 4 is attributed to the plastic deformation at the asperities during loading. When the stress was removed, the contact area at asperities did not return to the initial value. In Fig. 3 the gradual decrease means that plastic deformation occurred progressively upon cycling, due to the intermediate level of the stress amplitude; in Fig. 4 the abrupt decrease means that plastic deformation essentially occurred only in the first loading cycle, due to the higher stress amplitude. The leveling off of the resistance is attributed to the attainment of the maximum amount of plastic deformation at the corresponding stress amplitude. The higher stress amplitude, the smaller was the leveled off resistance and the smaller were the contact resistances at maximum and zero stresses; the higher the applied stress, the smoother was the surface upon loading, the less was the room for the contact area to be further decreased by loading, and the more was the contact area at maximum or zero stress.

The resistance at the maximum stress remained the same upon cycling at all three stress amplitudes; so did the shape of the resistance versus time curve of a cycle. This is due to the dominance of elastic deformation in the loaded state.

Concrete. Figure 5 shows the variation in resistance and stress during cyclic compressive loading at a stress amplitude of 5.0 MPa. The compressive strength of the mortar was 64 $\pm$2 MPa, as determined by compressive testing of 51$\times$51 $\times$51 mm (2$\times$2$\times$2 in) cubes. The stress-strain curve was a straight line up to failure. In every cycle, the resistance decreased as the compressive stress increased, such that the maximum stress

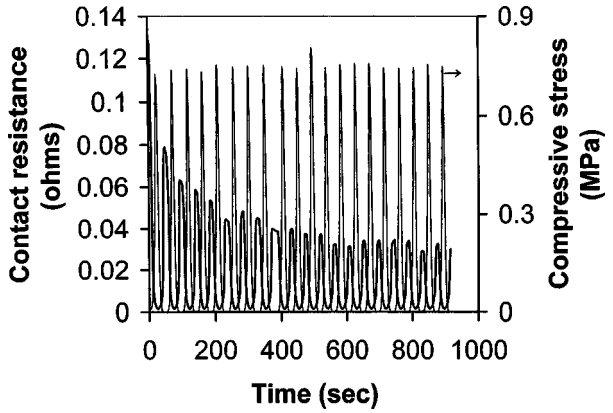

Fig. 3 Variation of contact resistance with time and of compressive stress with time during cycling compression of a graphite-graphite contact at a stress amplitude of 0.70 MPa

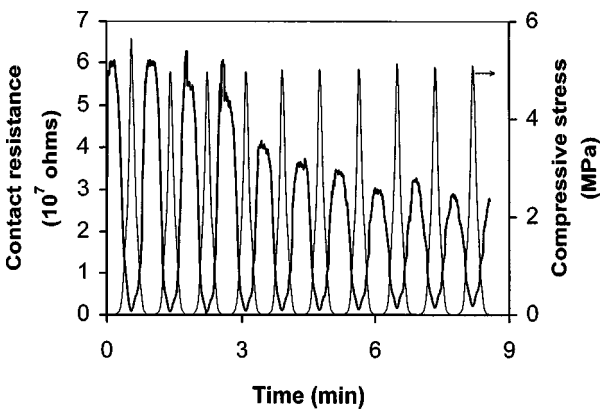

Fig. 5 Variation of contact resistance with time and of compressive stress with time during cycling compression of a mortar-mortar contact at a stress amplitude of 5 MPa

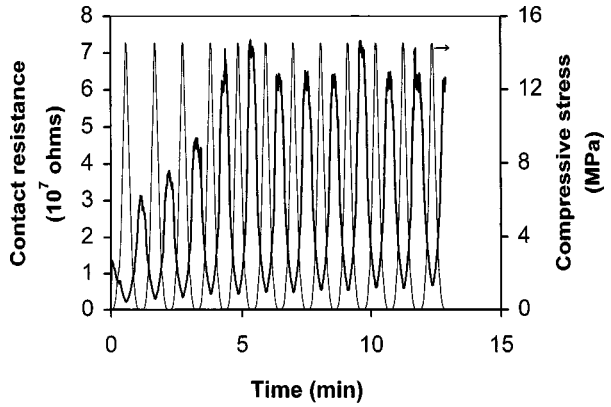

Fig. 6 Variation of contact resistance with time and of compressive stress with time during cycling compression of a mortar-mortar contact at a stress amplitude of 15 MPa

corresponded to the minium resistance and the minimum stress (zero stress) corresponded to the maximum resistance. The minimum resistance (at the maximum stress) increased slightly as cycling progressed, but the maximum resistance (at the minimum or zero stress) decreased with cycling. Due to the asperities at the interface, the local compressive stress on the asperities was much higher than the overall compressive stress. As a result, plastic deformation occurred at the asperities, which means more contact area was created during cycling. The occurrence of deformation is supported by the crosshead displacement observed within each cycle. The displacement was greatest (i.e., most deformation) at the maximum stress within each cycle and was not totally reversible. The plastic deformation is why the observed electrical resistance at the minimum stress (i.e., upon unloading) decreased as cycling progressed. On the other hand, due to the brittleness of the mortar, the compressive loading probably caused fracture at some of the asperities, thereby generating debris, which increased the contact resistance. Debris generation is probably the reason for the slight increase in the contact resistance at the maximum stress as cycling progressed. After about seven loading cycle, the maximum resistance (at the minimum stress) leveled off, due to the limit of the extent of flattening of the asperities. However, the slight increase of the minimum resistance (at the maximum stress) persisted beyond the first seven cycles, probably due to the continued generation of debris as cycling progressed.

The stress amplitude in Fig. 6 is 15.0 MPa, which is higher than in Fig. 5. The minimum resistance (at the maximum stress) increased with cycling more significantly than in Fig. 5. This is probably due to the more significant debris generation at the higher stress amplitude. The maximum resistance (at the minimum stress) increased in the first four cycles. This is probably due to the effect of debris generation overshadowing the effect of the flattening of the asperities. After four cycles, the maximum resistance essentially leveled off, probably due to the limit of the extent of debris generation for this stress amplitude.

The results of this work mean that, even at a low compressive stress amplitude of 5 MPa, the structure of a concrete-concrete contact changes during dynamic compression. Thus, the interfacial structure is dependent on the loading history. The debris generation at the interface may be of practical concern, as the load transfer between the contacting concrete elements may be affected by the debris.

Conclusion

Contact electrical measurement during cyclic compression was effective for studying the tribology of graphite and cement mortar. Elastic deformation and plastic deformation at asperities were distinctly observed through the reversible and irreversible decreases, respectively, of the contact resistance upon loading. Elastic deformation was dominant at the maximum stress. Plastic deformation progressed and then saturated upon stress cycling. In the case of cement mortar, debris generation was probably the cause for the increase of the contact resistance as stress cycling progressed.

References

[1] Chou, C. C., and Lin, J. F., 1997, ''Tribological Effects of Roughness and Running-In on Oil-Lubricated Line Contacts,'' Prod. Eng. (N.Y.), **211**, No. 3, pp. 209–222.

[2] Ackerman, C., Lentz, H., Powers, W., Jr., Jones, T., Casuccio, A., Spangler, C., Fischione, P., File, D., Anderson, G., Breindel, H., and Reed, B., 1990, ''Automated Torque and Resistance Measurements of Sliding Electrical Contacts During Life Testing,'' *Proc. 36th Annual IEEE Holm Conference on Electrical Contacts*, Illinois Inst. of Technology, Chicago, IL, pp. 259–268.

[3] Goodman, S. J. N., and Page, T. F., 1989, ''Contact Resistance and Wear Behavior of Separable Electrical Contact Materials,'' Wear, **131**, No. 1, pp. 177–191.

[4] Kostetskii, B. I., Gupka, B. V., Gorbanevskii, V. E., and Gupka, A. I., 1988, ''Investigation of Wear Relations by the Method of Contact Electrical Resistance,'' Sov. Eng. Res., **8**, No. 1, pp. 13–17.

[5] Bredell, L. J., Johnson, Jr., L. B., and Kuhlmann-Wilsdorf, D., 1987, ''Teaming Measurements of the Coefficient of Friction and of Contact Resistance as a Tool for the Investigation of Sliding Interfaces,'' Wear, **120**, No. 2, pp. 161–173.

[6] Braginskii, A. P., Evseev, D. G., Zdan'ski, A. K., and Kukol, N. P., 1985, ''Run-In Study Based on Electrical and Acoustic Characteristics,'' Sov. J. Friction Wear (Engl. Transl. Trenie i Iznos), **6**, No. 5, pp. 31–37.

[7] Marui, E., and Endo, H., 1992, ''Significance of Contact Resistance in Boundary Lubrication,'' Wear, **156**, pp. 49–55.

[8] Markova, L. V., Konchits, V. V., and Myshkin, N. K., 1995, ''Experimental Study of Metallic Contact Spots Formation,'' J. Friction Wear, **16**, No. 2, pp. 50–55.

[9] Shobert, E. I., 1965, *Carbon Brushes: The Physics and Chemistry of Sliding Contacts*, Chemical, New York, NY, pp. 185–186.

[10] Hounkponou, E., Nery, H., Paulmier, D., Bouchoucha, A., and Zaidi, H., 1993, ''Tribological Behavior of Graphite/Graphite and Graphite/Copper Couples in Sliding Electrical Contact: Influence of the Contact Electric Field on the Surface Passivation,'' Appl. Surf. Sci., **70–71**, No. 1–4, pp. 176–179.

[11] Duthie, F. W., 1985, ''Long Life Brushes—100 Years,'' *1985 Coil Winding Proceedings*, Int. Coil Winding Association, Minneapolis, MN, pp. 65–76.

[12] Rabinowicz, E., and Ross, A. Z., 1984, ''Compatibility Effects in the Sliding of Graphite and Silver-Graphite Brushes Against Various Ring Materials,'' *Electrical Contacts—1984, Proceedings of the Twelfth International Conference on Electric Contact Phenomena*, Meeting Jointly with the Thirtieth Annual Holm Conference on Electrical Contacts, Illinois Inst. of Technology, Chicago, IL, pp. 499–506.

[13] Konchits, V. V., 1984, ''Frictional Interaction and Current Passage in Composite-Metal Sliding Electrical Contact—II,'' Sov. J. Friction Wear (Engl. Transl. of Trenie i Iznos), **5**, No. 1, pp. 44–49.

[14] Milkovic, M., and Ban, D., 1996, ''Influence of the Pulsating Current Amplitude on the Dynamic Friction Coefficient of Electrographite Brushes,'' Carbon, **34**, No. 10, pp. 1207–1214.

[15] Bryant, M. D., and Burton, R. A., 1982, ''Frictional and Electrical Interactions in Current Collectors,'' Wear, **78**, pp. 49–58.

[16] Wu, Y., Zhang, G., and Tang, W., 1995, ''Research of Fiber/Graphite Composite Brush: Electrical Contacts,'' *Proceedings of the 41st IEEE Holm Conference on Electrical Contacts*, IEEE, Piscataway, NJ, pp. 315–322.

[17] Lu, C.-T., and Bryant, M. D., 1994, ''Simulation of a Carbon Graphite Brush with Distributed Metal Particles,'' IEEE Trans. Compon., Packag. Manuf. Technol., Part A, **17**, No. 1, pp. 68–77.

[18] Dillich, S., and Kuhlmann-Wilsdorf, D., 1983, ''Two Regimes of Current Conduction in Metal-Graphite Electrical Brushes and Resulting Instabilities,'' IEEE Trans. Compon., Hybrids, Manuf. Technol., **1**, pp. 45–54.

[19] Chen, P.-W., and Chung, D. D. L., 1993, ''Carbon Fiber Reinforced Concrete as a Smart Material Capable of Non-Destructive Flaw Detection,'' Smart Mater. Struct., **2**, pp. 22–30.